




# Miniatured Wide-Band Two-Element Monopole MIMO Antenna for 5G N38, N77 and N79 Bands Communication

Chandrasekhar Rao Jetty<sup>1</sup> , Shaik Sameer<sup>1</sup>, Kancherla Ajita Lakshmi<sup>2</sup>, V. N. Koteswara Rao Devana<sup>3</sup>, Varikallu Sirisha<sup>1</sup>, and Neelam Manikanta<sup>1</sup>

<sup>1</sup> Department of ECE, Bapatla Engineering College, Bapatla 522102, Andhra Pradesh, India  
jettychandu@gmail.com

<sup>2</sup> Department of ECE, Shri Vishnu Engineering College for Women (Autonomous), Bhimavaram, Andhra Pradesh, India

<sup>3</sup> Department of ECE, Aditya Engineering College, Surampalem, Kakinada, Andhra Pradesh, India

**Abstract.** A miniatured two-port wide-band MIMO antenna is presented in this work for use in 5G communications. The antenna measures 24 mm × 36 mm × 1.6 mm ( $0.2\lambda \times 0.3\lambda \times 0.0133\lambda$ ) and developed on FR-4 dielectric. The MIMO design composed of up of a multi-slotted circular two-element radiating patch and an I-shaped defected ground plan. To create the required operating bands at 2.5 GHz, 3.8 GHz, and 4.9 GHz frequencies, the radiating patch is carved with a circle-shaped slot, a crescent-moon-shaped slot, and a rectangle slot in the ground. The designed antenna operates at 2.5 GHz (N38: 2.35–3.0 GHz), 3.8 GHz (N77/N78: 3.3–4.4 GHz), and 4.9 GHz (N79: 4.7–5.5 GHz) with respectable impedance matching. The usage of a rectangular stub with minor protrusions and slots increases the MIMO antenna's impedance and isolation performance of more than 15 dB. Moreover, the antenna offers omnidirectional patterns, stable gain and efficiency, envelop correlation coefficient (ECC) of lower than 0.00001, diversity gain of 10, mean effective gain of  $-3$  dB across the functional bands. The findings demonstrate that the suggested architecture is a strong contender for 5G sub-6 GHz applications.

**Keywords:** Circular-slotted patch · I-shaped defected ground · 5G sub-6 GHz · Isolation · Multiple-input multiple-output · Wireless communication

## 1 Introduction

The extensive adoption of wireless systems has spurred a growing prerequisite for faster data speeds, reduced latency, and more effective spectrum usage, particularly in portable devices. Fifth generation (5G) wireless communication technology has debuted, offering various advantages over existing fourth-generation (4G) technology, including reduced latency, quicker transfer rates, and improved spectrum utilization. Specifically, 5G networks support 10 times faster data throughput than 4G networks. Three bands have been

established by the FCC for the 5G spectrum such as the lower, the sub-6 GHz, and the mmwave bands [1–4].

A possible solution for 5G systems to satisfy the wireless communication demands the multiple input multiple output (MIMO) technology. It can increase data throughput, spectrum utilisation, spatial variety and pattern diversity, and signal dropout without utilizing extra spectrum or transmit power [5]. In a MIMO network, several antennas are used at each end of the communication channel. When several antennas are installed on a dielectric, the MIMO antenna's compactness is a critical concern. Mutual coupling happens in array systems such as MIMO when distinct antenna elements are close enough to interact electromagnetically. As a result, as compactness increases or element spacing reduces, the potential of mutual coupling increases, reducing the performance of MIMO antennas because of power losses in a densely distributed environment. In order to develop a small MIMO antenna, a viable isolation method is essential. A considerable study has already showed on isolation enhancement in multi-antenna MIMO networks [6–16].

Some of the methods for reducing mutual coupling involve: employing a wide-band neutralization line [6], use of frequency-selective surface walls [7], utilization of two split-ring resonators (SRR) of different sizes [8], coupled resonators and wideband decoupling structures for two elements [9, 10], protruding strips in the shape of a rectangle and slotted T shape stubs [11], placing the defective ground structure with the T-shape stub on ground [12], the addition of parasitic components [13], the use of a shared ground branch as a decoupling mechanism amongst nearby antennas [14], and adaption of T shape stub on ground [15], use of reflector between the antennas [16]. Although the existing antennas in the prior art have complex antenna designs and are large in size, they offer sufficient isolation. For 5G sub-6 GHz applications, a compact MIMO design providing improved isolation is therefore essential.

In this research, a novel miniature two-port MIMO antenna design is recommended for sub-6 GHz application. The antenna measures  $24 \text{ mm} \times 36 \text{ mm} \times 1.6 \text{ mm}$  fed by  $50 \Omega$  microstrip line and is made of FR-4 dielectric material with a relative permittivity of 4.4 and a dielectric loss-tangent of 0.02. The designed antenna comprises of a multi-slotted circular shaped two-element radiating patch and I-shaped defected ground. A circle shaped slot and a crescent-moon shape cut on radiating element and rectangle slot in the ground plane are engraved to generate the required operating bands at 2.5 GHz, 3.8 GHz and 4.9 GHz frequencies. The MIMO antenna's impedance and isolation performance are improved by using a rectangular stub with minor protrusions and slots. Along with steady radiation patterns, less ECC, good DG, and adequate MEG, it also provides acceptable gain and efficiency.

## 2 Wide-Band MIMO Antenna Design

Figure 1 (a) and (b) depicts a compact two-port slotted circular MIMO antenna is developed for 5G sub-6 GHz N38, N78, N79 band applications. All parameters are expressed in millimeters. The proposed antenna is made of FR4-epoxy dielectric substrate material and measures  $24 \text{ mm} \times 36 \text{ mm}$  ( $0.2\lambda \times 0.3\lambda$ , where  $\lambda$  is computed at lowest cutoff frequency). The height of the substrate = 1.6 mm, the relative permittivity = 4.4, and

the loss-tangent = 0.02. CST Studio is used to create the suggested antenna design, optimize its dimensions, and simulate. The presented antenna comprises of a multi-slotted circular shaped two-element radiating patch on top of dielectric material and I-shaped defected ground on bottom as shown in Fig. 1 (a) and (b).

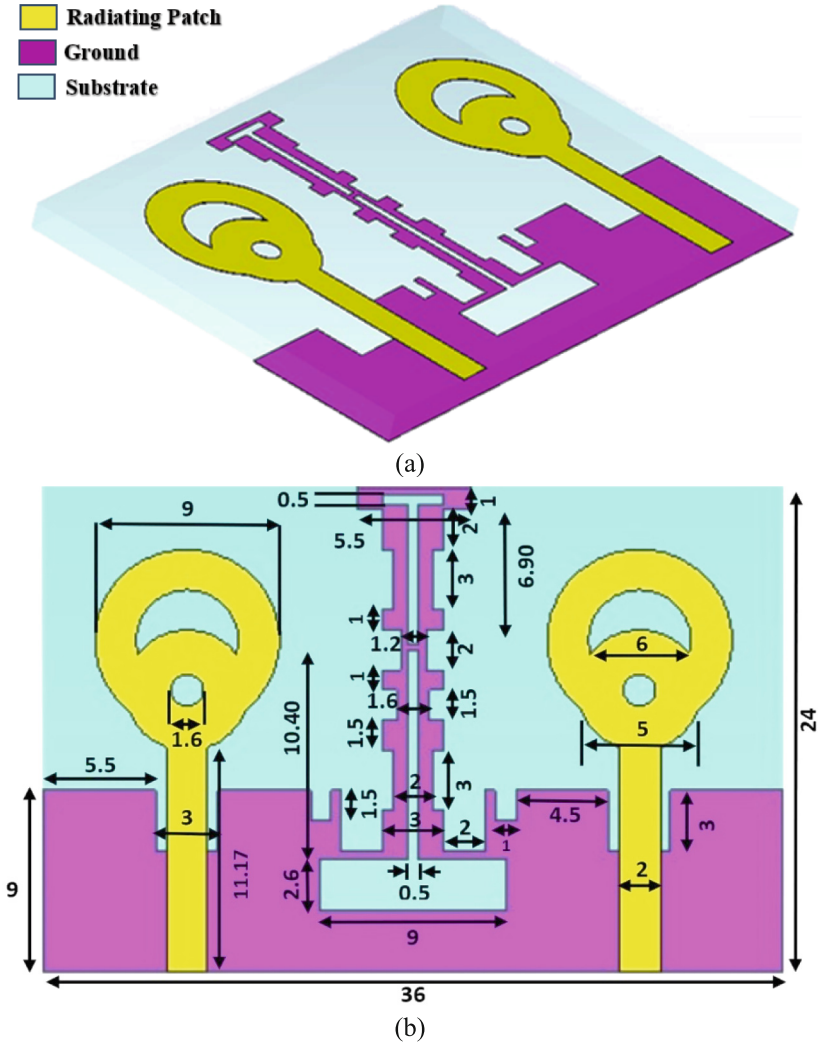


Fig. 1. Two-port MIMO Antenna; (a) dimetric view, (b) design with dimensions.

Initially, the circular shaped radiating patch of diameter 9 mm is fed by 2 mm × 11.17 mm microstrip line. A circular slot with diameter 6 mm is cut from the main circular patch and hence circular slotted patch is formed. Later, another circular patch of dimensions 5 mm is placed on the slotted patch and 1.6 mm diameter circular slot is etched to form proposed multi-slotted radiating patch. Therefore, a circle shaped slot

with a diameter of 1.6 mm and a crescent-moon shaped slot of 6 mm are etched from the radiating patch to generate the operating bands at N38 (2.6–3.0 GHz) and N79 (4.7–5.5 GHz) frequencies. The MIMO antenna ground is the defected ground of size 9 mm × 36 mm. The rectangular slot of size 2.6 mm × 9 mm is used on the ground plane to generate another frequency band at N77/N78 (3.3–4.4 GHz) band. The impedance matching at the created resonant bands is improved by incorporating slots and protrusions to the ground plane. All radiating elements are located 6mm away from the edge of the substrate. The isolation among the radiators is improved by arranging the radiating elements with appropriate spacing of 20 mm and the use of I-shaped defected ground stub.

### 3 Result Analysis

The two-port MIMO antenna's impedance characteristics are represented as  $S_{ii}$ , where  $i$  is an integer among 1 and 2, and  $S_{ij}$  ( $i \neq j$ ), which indicates the isolation or mutual coupling aspects of the antenna, where  $i$  and  $j$  are integers between 1 and 2 as revealed in Fig. 2 (a) and 2(b). The recommended design functions at 2.5GHz having  $S_{11}$  of -30

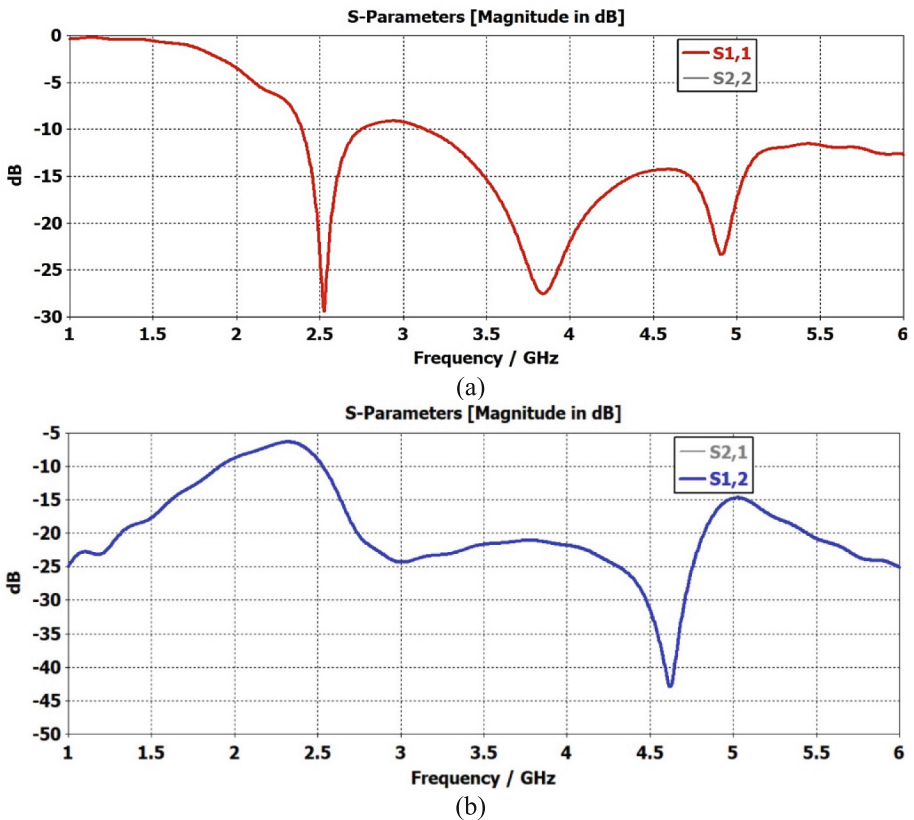
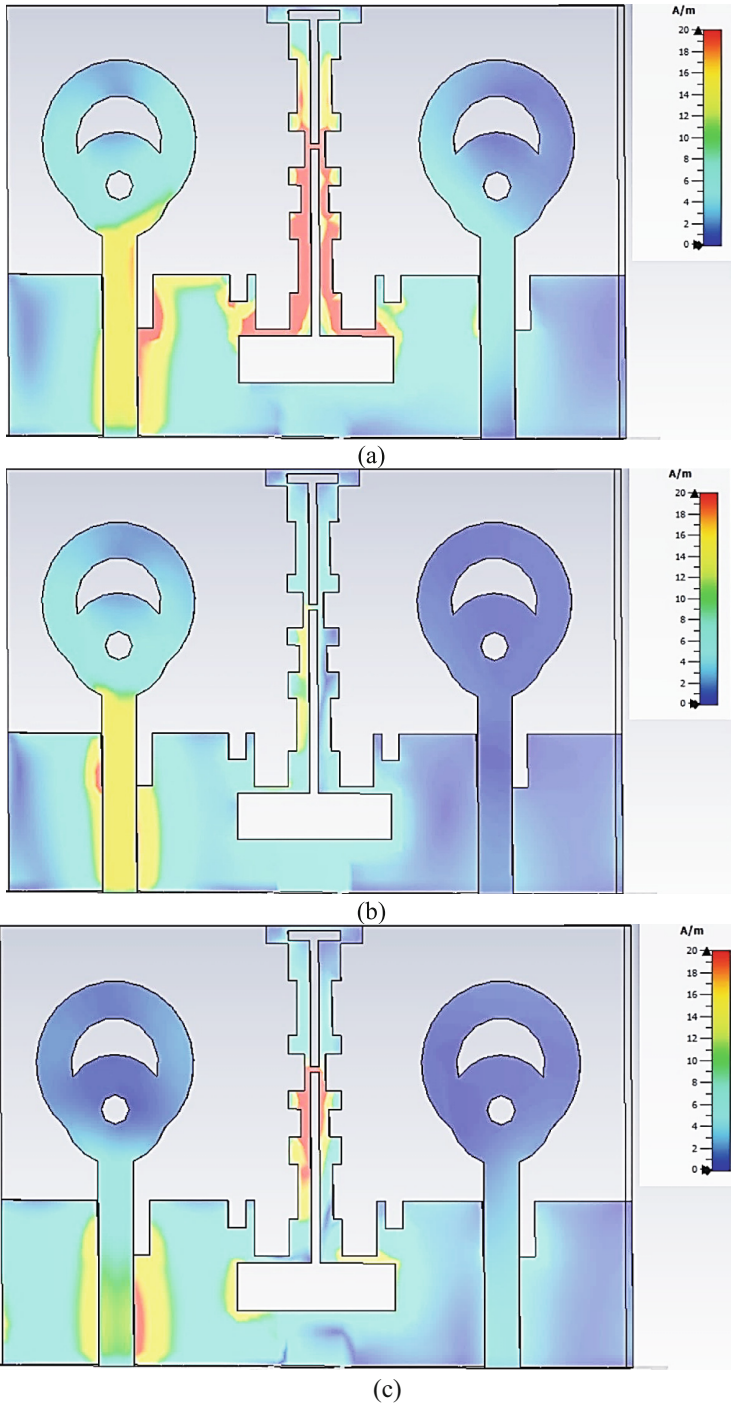


Fig. 2. Two-port MIMO Antenna S-parameter results.



**Fig. 3.** Surface current distribution at: (a) 2.5 GHz, (b) 3.8 GHz, and (c) 4.9 GHz.

dB, 3.8 GHz with  $S_{11}$  of  $-27.5$  dB, and 4.9 GHz with  $S_{11}$  of  $-24$  dB, cover N38, N77, and N79 bands. Furthermore, the suggested MIMO antenna has a high isolation  $S_{ij}$ , i.e.,  $S_{12}/S_{21}$ , of more than 15 dB throughout the operational band between all antenna ports. Figure 3 (a) to 3(c) describes the isolation performance of the MIMO design using I-shaped ground stub. It can be found that the MIMO antenna with I-shaped ground stubs among antenna elements efficiently prevents surface wave propagation and surface currents, improving isolation across antenna ports.

Figure 4(a) through 4(d) shows 2D E- and H-plane patterns at 2.5 GHz, 3.8 GHz, and 4.9 GHz. The antenna appears to offer both bidirectional E-plane and omnidirectional H-plane patterns within the working bands.

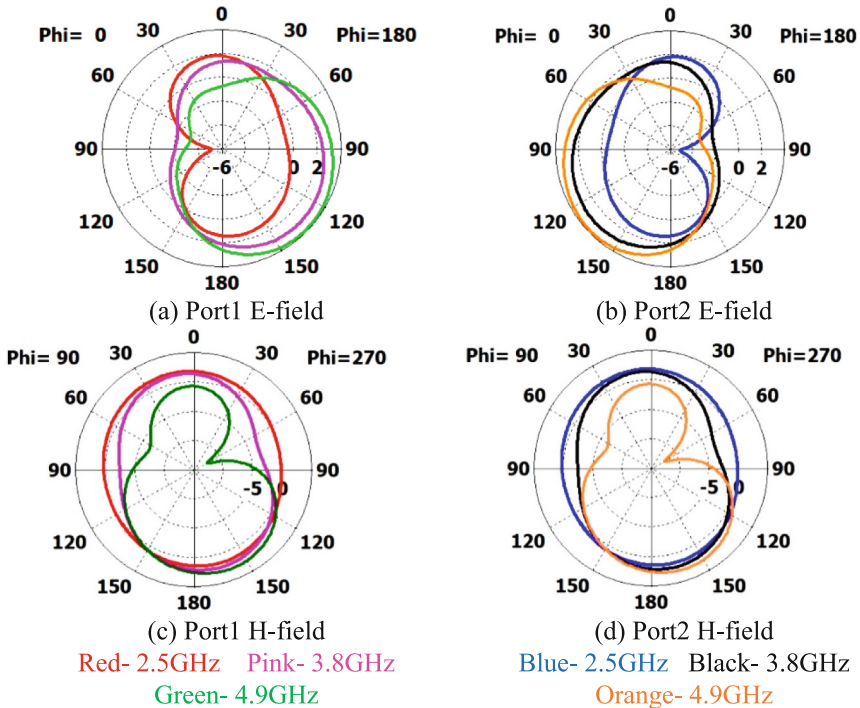


**Fig. 4.** Two-port MIMO Antenna 2D radiation patterns

The diversity features of the two-element MIMO design are revealed in Fig. 5(a) to 5(e). The suggested antenna element provides a consistent gain and total efficiency of 1.5 to 2.2 dBi and 81%, respectively, at the operating band of 2.5 GHz, 3.8 GHz and 4.9 GHz as shown in Fig. 5(a) and Fig. 5(b). The envelope correlation coefficient (ECC), which designates the total degree of similarity among the radiated fields of the various components in the MIMO antenna, is one of the most important MIMO diversity features. For a practical ECC requirement, it should be much lower than 0.5. Figure 5(c) displays that the modeled ECC is attained across the band at less than 0.00001, which is much less than the 0.5.

An additional parameter that can be used to assess the effectiveness of antenna diversity techniques is diversity gain (DG), where 10 is the ideal value and is attained by the proposed antenna as observed in Fig. 5(d). Another diversity measurement called mean effective gain (MEG) used to measure an antenna capability to recognize electromagnetic radiation in a multipath situation. According to Fig. 5(e), the planned MIMO antenna obtains a MEG of  $-3$  dB at the working bands. The ECC, DG and MEG parameters are calculated using the formulas found in [17, 18].

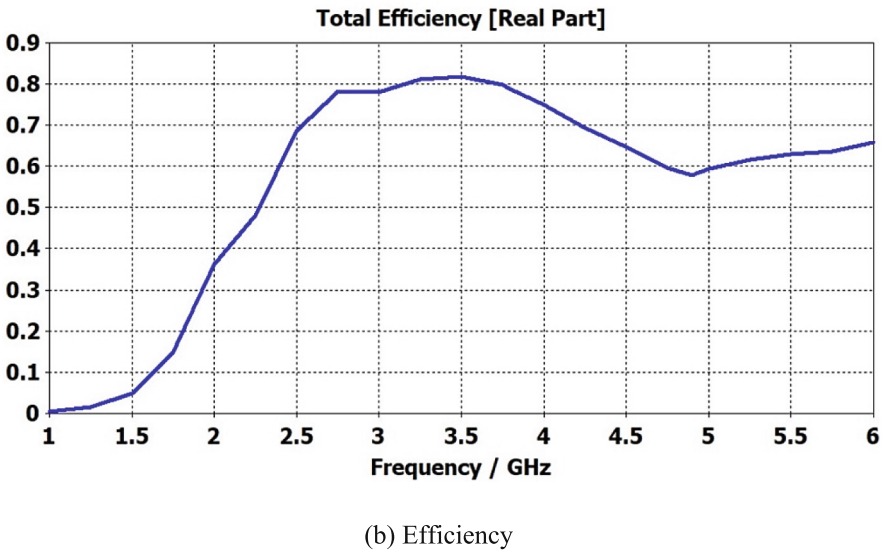
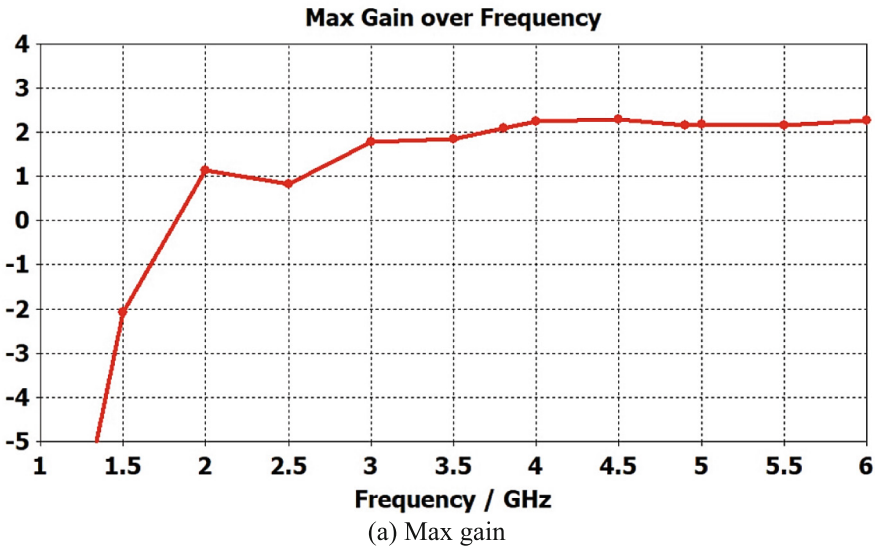
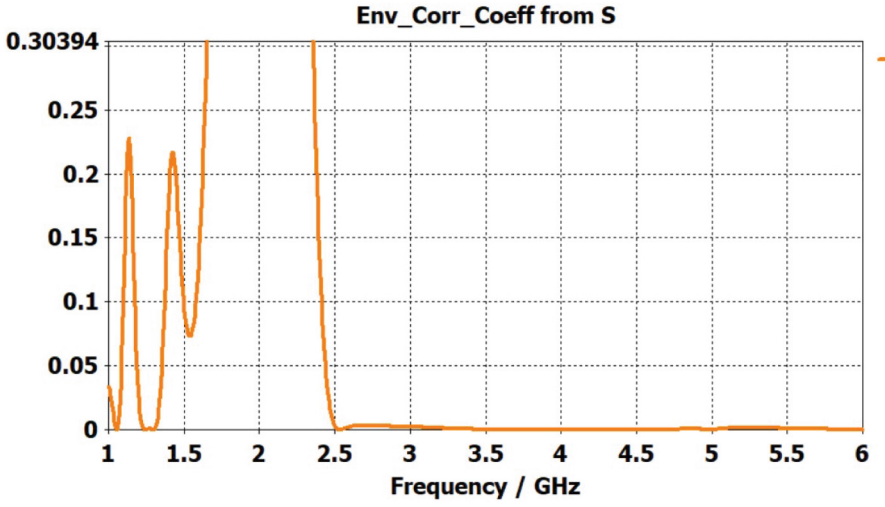
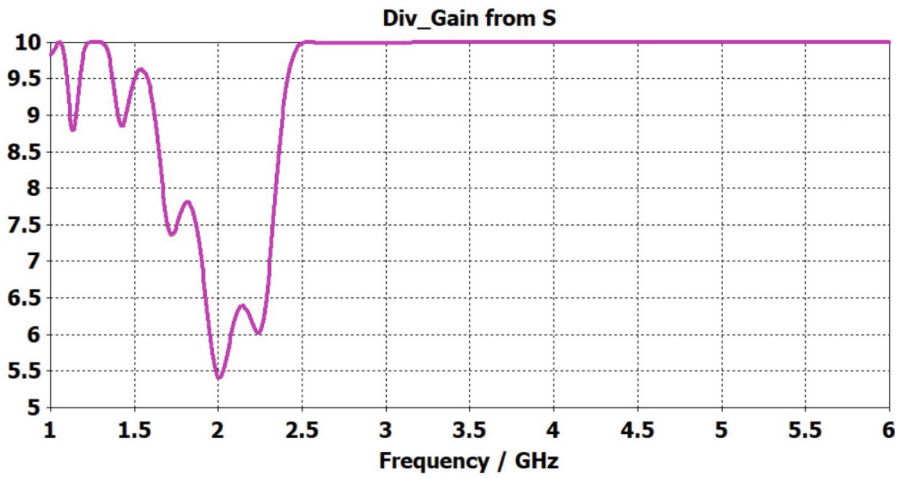


Fig. 5. Two-port MIMO Antenna parameters.

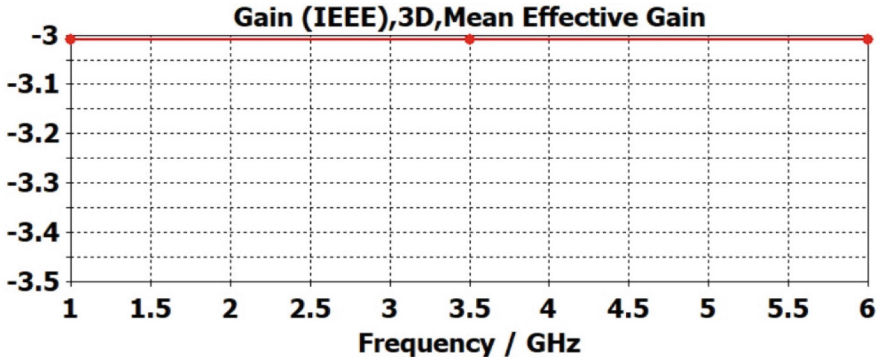


(c) ECC



(d) Diversity gain

Fig. 5. (continued)



(e) MEG

Fig. 5. (continued)

Table 1 compares and illustrates the suggested two-port MIMO antenna’s performance with that of other existing antennas with respect to antenna elements, size, gain, isolation, and MIMO diversity factors. The recommended design surpasses conventional antennas in terms of impedance bandwidth, isolation, RE, and ECC.

Table 1. Comparison between the designed antenna and prior antennas.

Ref.	No. of Elements	Size (in mm <sup>3</sup> )	Bands (GHz)	Isolation (dB)	R.E (%)	ECC
[11]	2	16 × 26 × 1.6	2.82–14.45	>20	>80	<0.08
[12]	2	18 × 21 × 0.8	2.8–12.2	>21	>80	<0.013
[13]	2	23 × 19 × 0.406	3.3–3.6, 4.8–5	>20	>71	<0.3
[14]	2	150 × 75 × 0.8	3.4–3.6, 4.8–5.0	>17.5	>70	<0.14
[15]	2	55 × 38 × 1.6	3.1–4.5	>20	>80	0.0004
<b>Prop.</b>	2	24 × 36 × 1.6	2.5, 3.8, 4.9	>15	>80	<0.00001

## 4 Conclusions

This research presents a small two port MIMO architecture for sub-6 GHz 5G applications. The antenna of  $24 \text{ mm} \times 36 \text{ mm} \times 1.6 \text{ mm}$  excited microstrip line is developed on FR-4 dielectric. The MIMO antenna design consists of a multi-slotted circular two-element radiating patch and an I-shaped defective ground. A circle-shaped slot and a crescent-moon-shaped slot on the radiating patch and rectangular slot in the ground plane are etched from the radiating patch to create the necessary operating bands at 2.5 GHz, 3.8 GHz, and 4.9 GHz frequencies. The use of a rectangular stub with modest protrusions and slots improves the MIMO antenna's impedance and isolation performance. Along with consistent radiation patterns, minimal ECC, good DG, and appropriate MEG, it offers acceptable gain and efficiency. Good performance of the antenna makes it a promising contender for 5G sub-6 GHz N38, N77, and N79 band transmissions.

## References

1. Rappaport, T.S., Xing, Y., MacCartney, G.R., Molisch, A.F., Mellios, E., Zhang, J.: Overview of millimeter wave communications for fifth-generation (5G) wireless networks-with a focus on propagation models. *IEEE Trans. Antennas Propag.* **65**(12), 6213–6230 (2017)
2. Cisco Visual Networking Index: Global mobile data traffic forecast update, 2015–2020. Cisco white paper, p. 9 (2016)
3. FCC takes steps to make millimeter wave spectrum available for 5G, Federal Communications Commission (2019). <https://www.fcc.gov/document/fcc-takes-steps-make-millimeter-wave-spectrum-available-5g>
4. Busari, S.A., Mumtaz, S., Al-Rubaye, S., Rodriguez, J.: 5G millimeter-wave mobile broadband: Performance and challenges. *IEEE Commun. Mag.* **56**(6), 137–143 (2018)
5. Foschini, G.J., Gans, M.J.: On limits of wireless communications in a fading environment when using multiple antennas. *Wirel. Pers. Commun.* **6**(3), 311–336 (1998)
6. Zhang, S., Pedersen, G.F.: Mutual coupling reduction for UWB MIMO antennas with a wideband neutralization line. *IEEE Antennas Wirel. Propag. Lett.* **15**, 166–169 (1998)
7. Karimian, R., Kesavan, A., Nedil, M., Denidni, T.A.: Low-mutual-coupling 60-GHz MIMO antenna system with frequency selective surface wall. *IEEE Antennas Wirel. Propag. Lett.* **16**, 373–376 (2016)
8. Xu, Z., Zhang, Q., Guo, L.: A compact 5G decoupling MIMO antenna based on split-ring resonators. *Int. J. Antennas Propag.*, 1–10 (2019)
9. Zhao, L., Yeung, L.K., Wu, K.L.: A coupled resonator decoupling network for two-element compact antenna arrays in mobile terminals. *IEEE Trans. Antennas Propag.* **62**(5), 2767–2776 (2014)
10. Pan, B.C., Cui, T.J.: Broadband decoupling network for dual-band microstrip patch antennas. *IEEE Trans. Antennas Propag.* **65**(10), 5595–5598 (2017)
11. Addepalli, T., Anitha, V.R.: A very compact and closely spaced circular shaped UWB MIMO antenna with improved isolation. *AEU Int. J. Electron. Commun.* **114**, 153016 (2020)
12. Jetti, C.R., Nandanavanam, V.R.: Trident-shape strip loaded dual band-notched UWB MIMO antenna for portable device applications. *AEU Int. J. Electron. Commun.* **83**, 11–21 (2018)
13. Li, Z., Du, Z., Takahashi, M., Saito, K., Ito, K.: Reducing mutual coupling of MIMO antennas with parasitic elements for mobile terminals. *IEEE Trans. Antennas Propag.* **60**(2), 473–481 (2011)

14. Ren, Z., Zhao, A.: Dual-band MIMO antenna with compact self-decoupled antenna pairs for 5G mobile applications. *IEEE Access* **7**, 82288–82296 (2019)
15. Agrawal, N., Gupta, M., Chouhan, S.: Modified ground and slotted MIMO antennas for 5G sub-6 GHz frequency bands. *Int. J. Microw. Wirel. Technol.* **15**(5), 817–825 (2023)
16. Maurya, N.K., Bhattacharya, R.: CPW-fed dual-band compact yagi-type pattern diversity antenna for LTE and WiFi. *Prog. Electromagn. Res. C* **107**, 183–201 (2021)
17. Addepalli, T., Kumar, M.S., Jetti, C.R., Gollamudi, N.K., Kumar, B.K., Kulkarni, J.: Fractal loaded, novel, and compact two-and eight-element high diversity MIMO antenna for 5G Sub-6 GHz (N77/N78 and N79) and WLAN applications, verified with TCM analysis. *Electronics* **12**(4), 952 (2023)
18. Glazunov, A.A., Molisch, A.F., Tufvesson, F.: Mean effective gain of antennas in a wireless channel. *IET Microw. Antennas Propag.* **3**(2), 214–227 (2009)